

## Interplay of disorder and interactions in the bilayer band insulator: A determinant quantum Monte Carlo study

Yogeshwar Prasad<sup>1,2,\*</sup> and Hunpyo Lee<sup>2,†</sup>

<sup>1</sup>Center for Condensed Matter Theory, Department of Physics, Indian Institute of Science, Bangalore 560012, India

<sup>2</sup>Department of Liberal Studies, Kangwon National University, Samcheok 25913, Republic of Korea

 (Received 7 September 2023; revised 8 January 2024; accepted 22 January 2024; published 14 February 2024)

In previous studies of the half-filled bilayer attractive Hubbard model [Prasad *et al.*, *Phys. Rev. A* **89**, 043605 (2014); Prasad, *Phys. Rev. B* **106**, 184506 (2022)], it has been shown that the clean system has a band-insulator (BI) to superfluid (SF) quantum phase transition. In this paper, we append the effects of random on-site disorder on the kinetic energy, double occupancy, and the pair-pair correlations in the bilayer model. Using the determinant quantum Monte Carlo simulation, we observe that the on-site random disorder plays a significant role in the localization of on-site pairs, and hence in the reduction of the effective hopping. This results in an increase of the double occupancy, which is an effect that is similar to the attractive interaction. We find no change in the critical value of the interaction at which the model undergoes a transition from the BI to SF regime, even though the pair-pair correlations get suppressed for finite on-site disorder strengths  $V_d/t = 0.1-0.8$ . We also confirm that the weak-disorder suppresses the SF phase largely in the strong-coupling limit. Hence the region of the SF phase reduces in the presence of random on-site disorder. Finally, through finite-size scaling, we have estimated the critical disorder strength  $V_d^c/t \sim 1.44$  at  $|U|/t = 5$ .

DOI: [10.1103/PhysRevB.109.064506](https://doi.org/10.1103/PhysRevB.109.064506)

### I. INTRODUCTION

Anderson [1] argued that the disorder in the absence of any interaction leads to the localization of the electronic states. On the other hand, the attractive interaction between the electrons lead to superconductivity, a very good example of the long-range order in physics. The competition between the superconductivity and the localization raises profound questions in condensed matter physics. The interplay of the effects of the interactions and the localization results in the destruction of the superconductivity with an increasing disorder and this leads to the superconductor-insulator (SI) [2,3] or superconductor-metal transition [4,5]. Earlier it was recognized that *s*-wave superconductivity is remarkably robust against weak disorder [1,6]. It has also been argued that the superfluid (SF) phase can survive even when single-particle states are localized by disorder [7]. Also, the *s*-wave superconductivity in two coupled Hubbard chains is more resistant to disorder than in the one-chain case [8]. In spite of the decades of research, a generally accepted physical picture of how the SF state is destroyed and the nature of the SI transition have not yet been understood. Ultracold atomic gases in optical lattices offer an opportunity to emulate these fundamental issues. The disorder in an optical lattice can be introduced [9] using the optical speckle [10–14], impurities [15], or a quasiperiodic optical lattice [16,17].

Motivated by the recent developments in the realization of an attractive Hubbard model on optical lattices [18,19], we

investigate the interplay between the on-site random disorder and the attractive interaction on the long-range pair-pair correlations in the two-dimensional bilayer band-insulator (BI) model at half filling. The bilayer BI model has been studied earlier in the absence of any disorder, both with on-site attractive Hubbard interaction [20,21] and repulsive Hubbard interactions [22,23], via quantum Monte Carlo and cluster dynamical mean-field approaches. The quantum Monte Carlo studies for the disordered attractive Hubbard model have been done in the past for a single-layer square lattice [3,24]. It has been found that in the single-layer attractive Hubbard model (AHM) at half filling in a square lattice, the superconducting order survives randomness out to a critical amount of disorder, but the charge ordering state is immediately destroyed [24].

In this work, we employ the exact and unbiased determinant quantum Monte Carlo (DQMC) technique to study the two-particle properties such as pair correlations in the bilayer BI (discussed in Refs. [20,21]) with random on-site disorder. The paper is organized as follows: In Sec. II, we briefly describe the bilayer BI model in the presence of the attractive Hubbard interaction with random on-site disorder. We also discuss the computational details of the DQMC technique used to investigate the model. In Sec. III, we investigate the effect of disorder on the double occupancy and the effective hopping, and on the two-particle pair-pair correlations. We also compare our results with the clean system. We find that the pair-pair correlation survives in the weak-disorder limit. The weak disorder suppresses the SF phase largely in the strong-coupling limit, whereas the effect of disorder on the pair-pair correlations is minimal in the weak-coupling limit. We perform scaling analysis to estimate the critical disorder strength required to destroy the SF phase. Finally, we

\*yogeshwar2609@kangwon.ac.kr

†hplee@kangwon.ac.kr

conclude by providing a phase diagram after summarizing our results in Sec. IV.

## II. MODEL AND COMPUTATIONAL METHOD

### A. Disordered bilayer band-insulator model

We start with a band-insulating state in the absence of any interaction such that the hoppings in both the layers of the bilayer square lattice are with opposite signs and the band gap is determined by the intralayer hopping, as studied in Refs. [20,21]. The Hamiltonian of the system in the presence of on-site random disorder is

$$\begin{aligned} \mathcal{H}_K &= \overbrace{-t \sum_{\langle ij \rangle, \sigma} (a_{i\sigma}^\dagger a_{j\sigma} + \text{H.c.}) - t' \sum_{\langle\langle i\bar{i}' \rangle\rangle, \sigma} (a_{i\sigma}^\dagger a_{i'\sigma} + \text{H.c.})}^{\text{A-layer}} \\ &+ \overbrace{+t \sum_{\langle ij \rangle, \sigma} (b_{i\sigma}^\dagger b_{j\sigma} + \text{H.c.}) + t' \sum_{\langle\langle i\bar{i}' \rangle\rangle, \sigma} (b_{i\sigma}^\dagger b_{i'\sigma} + \text{H.c.})}^{\text{B-layer}} \\ &- \underbrace{\sum_{i, \sigma} t_h(\mathbf{i}) (a_{i\sigma}^\dagger b_{i\sigma} + \text{H.c.}) - \mu \sum_{i, \sigma} (a_{i\sigma}^\dagger a_{i\sigma} + b_{i\sigma}^\dagger b_{i\sigma})}_{\text{A-B Layer hybridization}} \\ &+ \underbrace{\sum_{i \in A, \sigma} V_d(\mathbf{i}) a_{i\sigma}^\dagger a_{i\sigma} + \sum_{i \in B, \sigma} V_d(\mathbf{i}) b_{i\sigma}^\dagger b_{i\sigma}}_{\text{Disorder term}} \\ \mathcal{H}_U &= \underbrace{-U \sum_{\mathbf{i}} (a_{i\uparrow}^\dagger a_{i\downarrow}^\dagger a_{i\downarrow} a_{i\uparrow} + b_{i\uparrow}^\dagger b_{i\downarrow}^\dagger b_{i\downarrow} b_{i\uparrow})}_{\text{Interaction term}}. \end{aligned} \quad (1)$$

We recall that  $a_{i\sigma}^\dagger$  ( $b_{i\sigma}^\dagger$ ) and  $a_{i\sigma}$  ( $b_{i\sigma}$ ) are the creation and annihilation operators of spin- $\frac{1}{2}$  fermions with spin  $\sigma = \uparrow, \downarrow$  at site  $\mathbf{i}$  corresponding to the  $A$  layer ( $B$  layer) of the bilayer square lattice. Here,  $t$  is the nearest-neighbor hopping,  $t'$  is the next-nearest-neighbor hopping, and  $t_h$  is the interlayer hopping which hybridizes the  $A$  and  $B$  layers,  $U (> 0)$  is the attractive Hubbard interaction, and  $\mu$  is the chemical potential. The random potential  $V_d^{A/B}(\mathbf{i})$  is chosen independently at each site  $\mathbf{i}$ , belonging to layer  $A$  or  $B$ , from the uniform distribution  $[-V_d : V_d]$  that is symmetric about zero. According to the central limit theorem,  $\sum_{i=1}^N V_d(\mathbf{i}) = 0$ , where  $N$  being the total number of sites. The pure case corresponds to all on-site potentials vanishing [ $V_d(\mathbf{i}) = 0$ ].

### B. Brief description of determinant quantum Monte Carlo simulation

We begin by including the disorder term of the Hamiltonian in  $\mathcal{H}_K$  and applying the *Trotter-Suzuki* decomposition to separate the kinetic and the interaction energy exponentials [25,26]. With the addition of the disorder term in the kinetic energy (KE) term, the kinetic exponential will have the following expression:

$$e^{-\Delta\tau \mathcal{K}} = \prod_{\sigma} e^{-\Delta\tau \sum_{\alpha, \gamma} \sum_{\langle ij \rangle} (c_{i, \alpha, \sigma}^\dagger \mathbb{K}_{ij\alpha\gamma}^{\sigma} c_{j, \gamma, \sigma} + \text{H.c.})}, \quad (2)$$

where  $c_\alpha$ 's are equivalent to  $a$  and  $b$  operators for  $\alpha = 1$  and  $2$ , respectively, and  $\mathbb{K}$  is the modified KE matrix whose elements

are given by

$$\mathbb{K}_{ij\alpha\gamma}^{\sigma} = t_{ij} - [\mu - V_d(\mathbf{i}_\alpha)] \delta_{ij} \delta_{\alpha\gamma}, \quad (3)$$

with  $t_{ij}$  being the hopping matrix. The interaction exponential has the following expression:

$$e^{-\Delta\tau \mathcal{V}} = e^{-\Delta\tau \sum_{\alpha} \sum_i U n_{i\uparrow}^{\alpha} n_{i\downarrow}^{\alpha}}. \quad (4)$$

After applying the Hubbard-Stratonovich transformation for the bilayer band-insulator model, the elements of the matrix  $\mathbb{V}$  in the interaction exponential term are modified to

$$\mathbb{V}_{ij\alpha\gamma}^{\sigma} = -\frac{\lambda s_i}{\Delta\tau} \delta_{ij} \delta_{\alpha\gamma}, \quad (5)$$

with  $\cosh(\lambda) = e^{|\lambda| \Delta\tau/2}$  and  $s_i$  being the discrete Ising variables,  $s = \pm 1$ . At half filling,  $\mu$  is set as  $\mu = \frac{|U|}{2}$ . Following all the steps of the DQMC algorithm, we performed the simulation for our model at half filling for  $N = 2 \times L^2$  sites with the periodic boundary conditions. Here,  $L$  represents the number of sites in each direction of the square lattice. We choose the hopping  $t = 1$  to set our unit of energy.  $t'/t = 0.1$  and  $t_h/t = 0.6$  have been set to compare the results with the ‘‘clean’’ system studied in Refs. [20,21]. The inverse temperature has been discretized in small imaginary time intervals  $\Delta\tau t = 0.05$ , resulting in very small systematic errors ( $\sim \Delta\tau^2$ ) involved in these simulations. For  $|U|/t = 8$ , the  $\Delta\tau t = 0.025$  has been chosen to reduce fluctuations in the high-interaction regime. All the simulations have been done at temperature  $T/t = 0.1$  for a system size  $L = 16$ , unless specified otherwise. In all these calculations, disorder averages have been done over 300–400 disorder configurations, generated randomly from a uniform distribution as discussed, and the indicated error bars are the statistical error bars over these disorder averages of the Monte Carlo sampling.

## III. RESULTS

### A. Double occupancy and the pair formation

Figure 1 shows the evolution of the rescaled double occupancy  $\tilde{D}$  or the density of the on-site pairs defined as

$$\tilde{D} = \frac{D - \langle n_{i\uparrow} \rangle^2}{\langle n_{i\uparrow} \rangle - \langle n_{i\uparrow} \rangle^2} = 4D - 1,$$

with the random on-site disorder  $V_d/t$  for various system sizes. Here the double occupancy  $D = \frac{1}{N} \sum_{i, \alpha} \langle n_{i\uparrow}^{\alpha} n_{i\downarrow}^{\alpha} \rangle$ . The inset of Fig. 1 shows the plot of the  $\tilde{D}$  versus the attractive interaction  $|U|/t$  at temperature  $T/t = 0.1$ . We see that  $\tilde{D}$  is independent of the system size and it increases with the increase in the disorder strength and saturates to its maximum value for the large disorder strengths. At weak-disorder strengths ( $V_d/t \ll 1$ ),  $\tilde{D}$  increases slowly as the kinetic energy term dominates and favors delocalization, but in the intermediate disorder region ( $V_d/t \sim 1$ ), the random disorder potential competes with the KE term and hence enhances the pairing. As we go towards the large disorder region,  $\tilde{D}$  approaches its limiting value and hence saturates. Thus the random on-site disorder promotes  $\tilde{D}$ , the local pair formation, and hence the localization of pairs, i.e., the effect similar to the attractive interaction  $|U|/t$ . We see the existence of the molecule formation along the BCS-BEC crossover as we tune the attractive

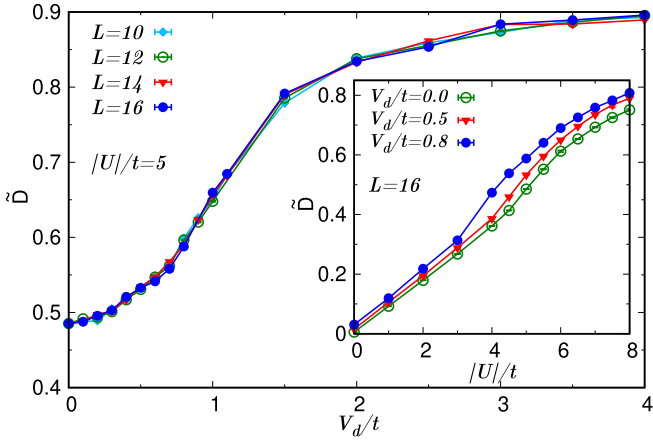


FIG. 1. The evolution of the rescaled double occupancy  $\tilde{D} = (4D - 1)$  with random on-site disorder  $V_d/t$  for various system sizes at the temperature  $T/t = 0.1$ . The system is at half filling, with interplane hybridization  $t_h/t = 0.6$ . Inset: The plot of the  $\tilde{D}$  vs the attractive interaction  $|U|/t$ .

interaction both in the absence and in the presence of the random disorder which comes from the evolution of the double occupancy (inset of Fig. 1). We see that the double occupancy increases from its noninteracting limit value ( $\tilde{D} \approx 0$ ) to its limiting value ( $\tilde{D} \approx 1$  at half filling) as  $|U|/t$  approaches infinity and the presence of the disorder enhances this pair formation process.

### B. Effective hopping

As we tune the disorder strength at finite attractive interaction, we expect the effective single-fermion transfer to decrease. Hence the local fermions tend to form pairs, resulting in the increase in the double occupancy, as seen earlier. A measure of this reduction in the single-fermion transfer is given by the effective hopping defined as

$$\frac{t_{\text{eff}}}{t} = \frac{\langle \mathcal{H}_K \rangle}{\langle \mathcal{H}_K \rangle_{V=0}}, \quad (6)$$

the ratio of KE at finite disorder to the kinetic energy at zero disorder at a given interaction strength  $|U|/t$ . In Fig. 2, we plot the effective hopping for various disorder strengths  $V_d/t$  at temperature  $T/t = 0.1$ . We see that the effective hopping declines as the attractive interaction  $|U|/t$  increases and the declination gets faster as we increase the disorder strength. Hence the disorder enhances the pairing and reduces the effective hopping due to the localization effects. We observe that the decrease in the effective hopping is very sharp in the strong-coupling limit (inset of Fig. 2) in the presence of disorder, where the system goes to the Bose-glass (BG) phase.

In Fig. 3, we have shown the evolution of KE and its derivative with respect to the attractive interaction  $|U|/t$  at disorder strength  $V_d/t = 0.5$ . We observe a peak at  $|U|/t = 5$  in the derivative of KE, which coincides with the critical strength  $|U_c|/t$ , calculated from the finite-size scaling analysis of the pair structure factor, which marks the transition from the BI to the SF state. In the inset of Fig. 3, we see that for the interaction strengths  $|U|/t \sim 0-2$ , the KE increases slowly, but

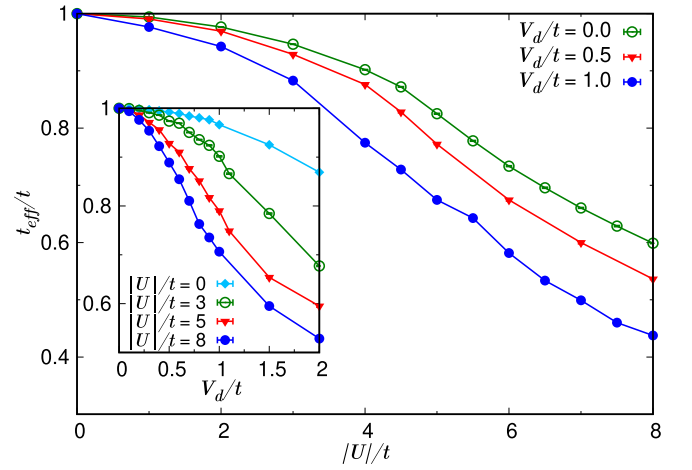


FIG. 2. The effective hopping  $t_{\text{eff}}/t$  as a function of the interaction strength  $|U|/t$  for various disorder strengths  $V_d/t$  at  $T/t = 0.1$ . As the interaction energy  $|U|/t$  increases, the effective hopping declines. Inset: The effective hopping as a function  $V_d/t$  for various  $|U|/t$  at the same temperature.

as we increase the interaction strength further, there is a sharp rise in the KE (or a sharp decrease in the effective hopping).

### C. Pair-pair correlations

In the following sections, we have studied the pair-pair and density-density correlations in the presence of random on-site disorder at half filling in the proposed bilayer band-insulator model. We find that the pair-pair correlation survives in the weak-disorder limit, while the density-density correlation function gets suppressed even with a slight increase in the disorder.

Figure 4 show the dependence of the ground-state pair-pair correlation functions, defined as

$$P_s^{\alpha\gamma}(\mathbf{i}, \mathbf{j}) = \langle \Delta_s(\mathbf{i}, \alpha) \Delta_s^\dagger(\mathbf{j}, \gamma) + \text{H.c.} \rangle, \quad (7)$$

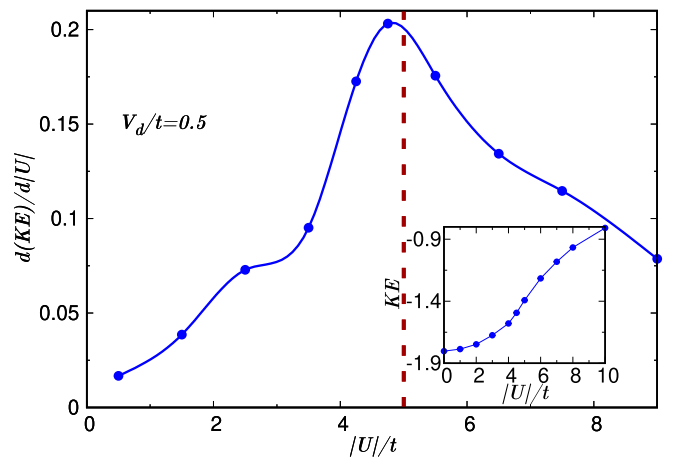


FIG. 3. The evolution of the kinetic energy (KE) and its derivative with respect to the attractive interaction  $|U|/t$  at disorder strength  $V_d/t = 0.5$ . In the intermediate-coupling regime, there is a sharp increase in the KE, which can be clearly seen in the derivative of KE where we observe a peak at  $|U|/t = 5$ .

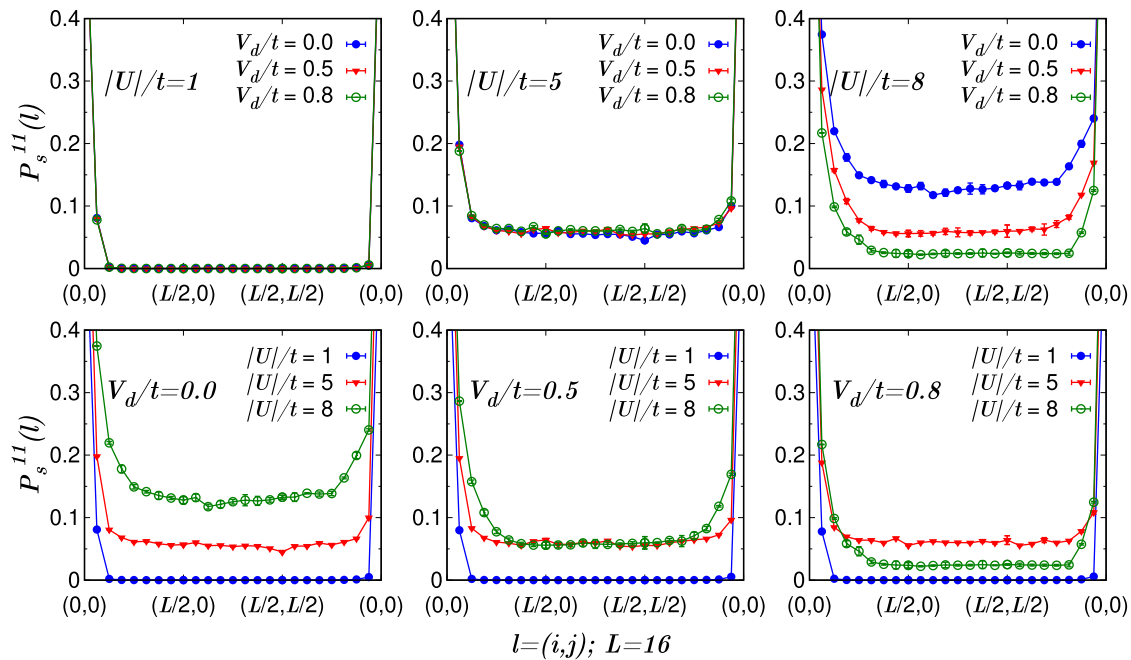


FIG. 4. The spatial dependence of the ground-state pair correlation functions  $P_s^{11}(l)$  for different disorder strengths  $V_d/t$  in a bilayer BI model at attractive interaction  $|U|/t = 1, 5,$  and  $8$  (top panels) and for different interaction strengths  $|U|/t$  at  $V_d/t = 0.0, 0.5,$  and  $0.8$  (bottom panels). The correlation functions converge to a nonzero value at large separations for  $|U|/t = 5$  and  $8$ , providing clear evidence for the long-range order even in the presence of random on-site disorder, though the value of the pair-pair correlations decreases with the increase in the disorder strength and goes to zero for  $V_d/t = 0.8$  at  $|U|/t = 8$ .

on separation  $\mathbf{i}$  for different combinations of the disorder strengths  $V_d$  and the attractive interactions  $|U|/t$  in the bilayer BI model at half filling. Here,  $\Delta_s(\mathbf{i}, \alpha) \sim c_{\mathbf{i}, \alpha \downarrow} c_{\mathbf{i}, \alpha \uparrow}$  and  $\Delta_s^\dagger(\mathbf{i}, \alpha)$  are the pair annihilation and creation operators. As mentioned earlier, the separation  $\mathbf{l} = (\mathbf{i}, \mathbf{j})$  follows a trajectory along the  $x$  axis to maximal  $x$  separation  $(\frac{L}{2}, 0)$  on a lattice with the periodic boundary conditions, and then to  $(\frac{L}{2}, \frac{L}{2})$  before returning to separation  $(0,0)$ . In the weak-coupling limit, there is no pair-pair correlation (shown in Fig. 4 for  $|U|/t = 1$ ) as the system remains in the BI. We see that the correlation functions converge to a nonzero value at large separations for  $|U|/t = 5$  in weak ( $V_d/t \ll 1$ ) and intermediate ( $V_d/t \sim 1$ ) disorder regimes, providing a clear evidence for the long-range order even in the presence of random on-site disorder. At  $|U|/t = 8$ , the pair correlation survives in the weak-disorder limit, but goes to zero for  $V_d/t = 0.8$ , indicating a transition from the SF to the BG phase where the fermionic pairs get localized in the strong-coupling and the strong-disorder limit. We observe that the pair correlations in the strong-coupling regime gets strongly suppressed as compared to the intermediate-coupling regimes. This reduces the SF region in the phase diagram. The existence of the long-range order for  $|U|/t \geq 5$  implies that the presence of the random on-site disorder does not change the critical value of the interaction strength  $|U_c|/t$ , which we confirm from the finite-size scaling analysis.

In Fig. 5, we show the evolution of the  $s$ -wave pair structure factor  $S_s$  with the disorder strength  $V_d/t$  for various system sizes for interaction  $|U|/t = 5$  at  $T/t = 0.1$ . We observe that in the weak-disorder limit, the pair structure factor increases slightly from its “clean” system (absence of disorder) value and then decreases sharply with the increase in the disorder

strength, finally saturating to a finite nonzero value which does not depend on the size of the lattice. It shows that the  $s$ -wave pair structure factor has a strong system-size dependence in the weak-disorder limit, indicating that the correlation length  $\xi$ , which depends on the disorder strength and temperature, is large compared to the lattice size  $L$ . The lattice-size dependence goes away as soon as  $\xi$  becomes small as compared to

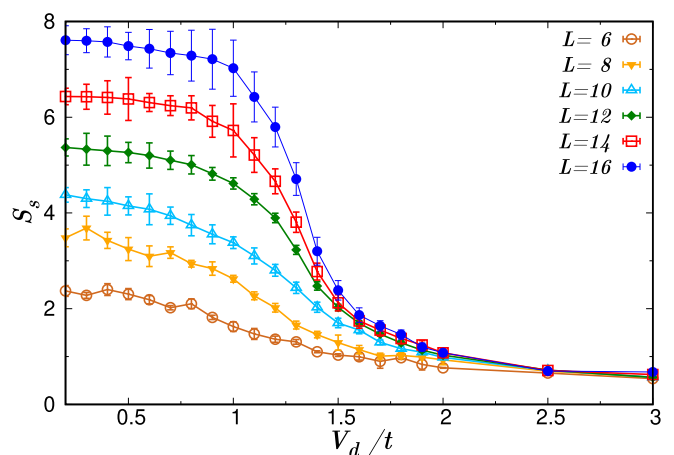


FIG. 5. The evolution of the  $s$ -wave pair structure factor  $S_s$  with the disorder strength  $V_d/t$  for different system sizes at interaction  $|U|/t = 5$ . In the weak-disorder limit,  $S_s$  almost remains constant. With the increase in the disorder strength,  $S_s$  slightly increases and then decreases sharply, finally saturating to a finite nonzero value which does not depend on the size of the lattice.  $S_s$  depends on the system size in the weak-disorder limit.

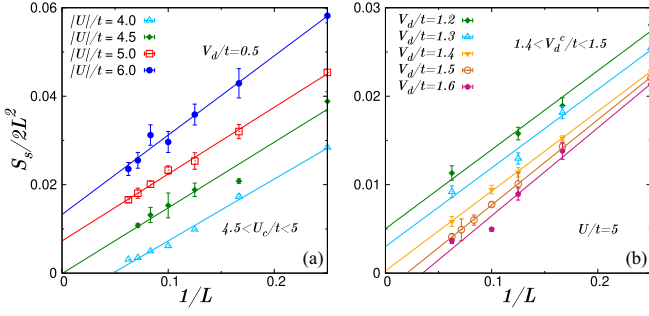


FIG. 6. Finite-size scaling of the  $s$ -wave pair structure factor  $S_s/2L^2$ . The symbols are the determinant quantum Monte Carlo results and the dashed lines are the extrapolation performed via a linear least-squares fit for (a) each  $|U|/t$  in presence of disorder  $V_d/t = 0.5$  and (b) each  $V_d/t$  at  $|U|/t = 5$ . The inverse temperature has been fixed at  $\beta t = 10$ . We observe that  $S_s$  vanishes for  $|U|/t < 4.5$  as  $L \rightarrow \infty$ . Thus,  $|U_c|/t$  lies in the range  $4.5 < |U_c|/t < 5$ .

$L$ , which gives the information about the short-range nature of the pair-pair correlation in the large disorder limit.

#### D. Scaling analysis

We have observed that our bilayer BI model displays the long-range order in the pair-pair correlations, even at intermediate disorder strengths. Hence, we expect the Huse's argument [27] of the "spin-wave scaling" to hold,

$$\frac{S_s}{2L^2} = \Delta_0^2|_V + \frac{C(U, V_d)}{L}, \quad (8)$$

where  $\Delta_0$  is the SF order parameter at zero temperature and disorder  $V_d/t$ , and  $C$  is a constant which depends on the interaction strength  $U/t$  and random on-site disorder  $V_d/t$ .

The SF order parameter  $\Delta_0$  can also be extracted from the *equal-time*  $s$ -wave pair-pair correlation function  $P_s(\mathbf{R})$  for the two most distant points on a lattice, i.e., having  $\mathbf{R} = (L/2, L/2)$  [3], with a similar spin-wave theory correction,

$$P_s(\mathbf{R}) = \Delta_0^2 + B(U, V_d)L. \quad (9)$$

Thus, we estimate the zero-temperature SF parameter from the finite-size scaling of the  $s$ -wave pair structure factor using Eq. (8) and Eq. (9), and hence estimate the zero-temperature critical value of the interaction at which our bilayer BI, in the presence of disorder, undergoes a transition to the SF state.

In Fig. 6, we present the finite-size scaling of the  $s$ -wave pair structure factor  $S_s/2L^2$  in the presence of the random disorder. It shows that the zero-temperature critical interaction  $|U|/t$  lies between 4.5 and 5.0 at the disorder strength  $V_d/t = 0.5$ , which is the same as is obtained in the absence of disorder in Ref. [21]. Hence the disorder does not affect the critical value, but plays a significant role in suppressing the pair correlation function.

In the strong-coupling limit, due to a large on-site attraction, the fermions form tightly bound pairs and can be treated as bosons which condense to form a SF phase. In this limit, we can map our attractive Hubbard model to the effective hard-core Bose-Hubbard model with repulsive next-nearest-neighbor interaction. The pair annihilation

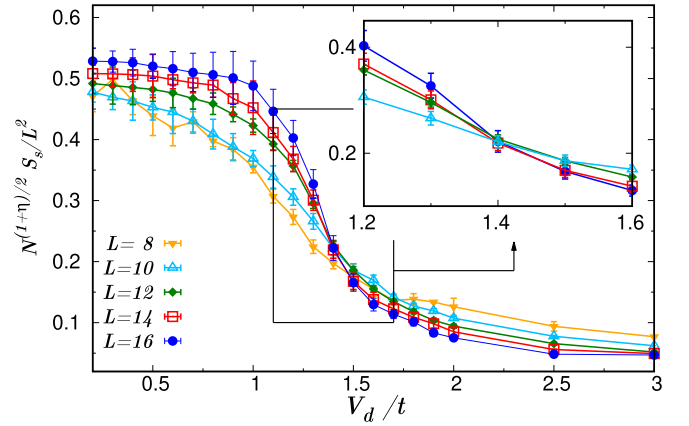


FIG. 7. Rescaled  $S_s$  as a function of the disorder strength  $V_d/t$  at  $|U|/t = 5$  for different system sizes. Inset: The enlarged region where the curves intercept each other, around  $V_d/t = 1.5$ – $2.0$ .

$[\Delta_s(\mathbf{i}, \alpha) \sim c_{i,\alpha\downarrow}c_{i,\alpha\uparrow}]$  and creation  $[\Delta_s^\dagger(\mathbf{i}, \alpha)]$  operators of our proposed model will be equivalent to the bosonic creation and annihilation operators ( $b_i^\dagger$  and  $b_i$ ). Thus we expect that in the presence of disorder, there exists a BG phase before the system goes to a CDW insulator state since, at half filling, in the strong-coupling limit, a hard-core Bose-Hubbard model exhibits a SF to BG transition with increasing disorder  $V_d/t$ . This transition belongs to the  $(d+1) - XY$  universality class [28].

To estimate the critical value of the disorder strength beyond which our system undergoes a SF to BG transition, we use the scaling ansatz used in Refs. [28,29],

$$L^{1+\eta} \frac{S_s}{L^2} = F[(V_d - V_c)L^{1/\nu}], \quad (10)$$

where  $\nu$  and  $\eta$  are the correlation length exponent and the order parameter exponent, respectively.  $V_c/t$  is the critical disorder strength required to destroy the superfluid order. At  $V_d/t = V_c/t$ , the rescaled pair structure factor becomes independent of the system size and hence all the curves for different system sizes must intercept each other at  $V_c/t$ .

Figure 7 shows the rescaled pair structure factor  $S_s$  as a function of the disorder strength  $V_d/t$  at  $|U|/t = 5$  for different system sizes. We observe that all the curves corresponding to different system sizes intersect each other at  $V_d^c/t \sim 1.4$ . The inset shows the enlarged region, around  $V_d/t = 1.1$ – $1.7$ , where the curves intersect each other. In Fig. 8, we plot the rescaled pair structure factor  $S_s$  versus the universal scaling function  $F(z)$  [Eq. (10)]. We observe that all the curves corresponding to different system sizes collapse to a single curve for  $\nu = 0.67$ ,  $\eta = 0.04$ , and  $V_d^c/t = 1.44$ , except in the weak-disorder regime. The perfect collapse of our data, for  $\nu = 0.67$  and  $\eta = 0.04$ , shows that the SF to BG transition lies in the universality class of the  $3D - XY$  model. The obtained critical disorder strength is roughly the same as the single-layer half-filled attractive Hubbard model where  $V_d^c/t \sim 1.5$  at  $|U|/t = 4$  [24].

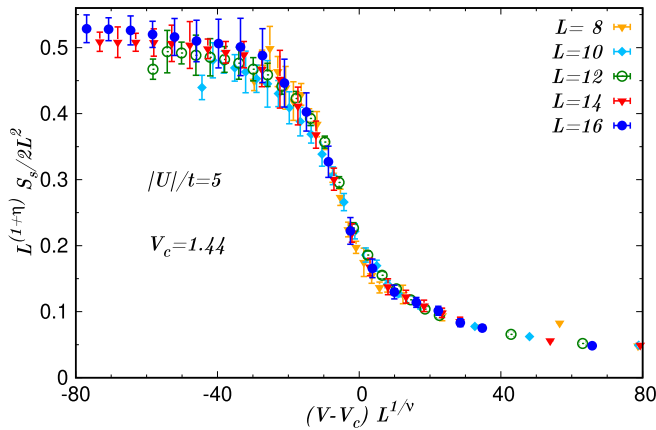


FIG. 8. Rescaled  $S_s$  plotted against  $|V_d - V_c^d| L^{1/\nu}$  at  $|U|/t = 5$  for different system sizes. All the data points of the various system sizes collapse into a single curve for  $\nu = 0.67$ ,  $\eta = 0.04$ , and  $V_c^d/t = 1.44$ .

### E. $V - U$ phase diagram of bilayer band insulator in the presence of disorder

Finally, we discuss a  $V - U$  phase diagram for the proposed bilayer BI model at finite hopping between the layers and in the presence of disorder, shown in Fig. 9. In the “clean” noninteracting case, as we tune disorder, we expect that the BI will eventually go to the Anderson-insulator state

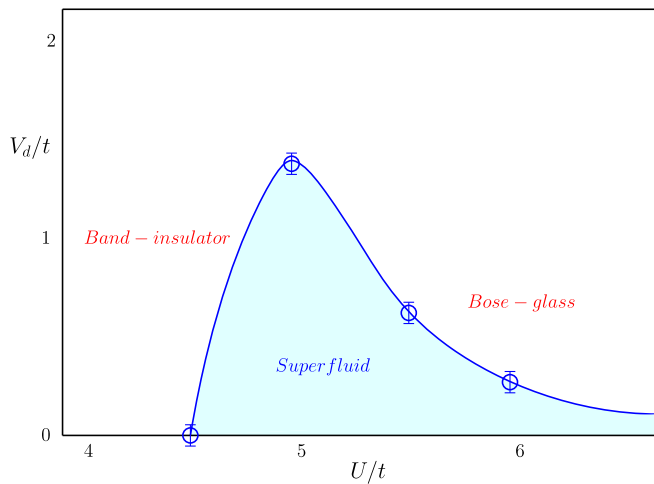


FIG. 9.  $V - U$  phase diagram of proposed bilayer band insulator (BI) in the presence of disorder at finite layer hybridization. In the absence of disorder, the system goes to a superfluid (SF) phase from the BI phase as we tune the interaction. In the strong-coupling limit, it goes to a “bosonic” charge density wave (CDW) phase. As we tune the disorder, the BI phase is expected to go to an Anderson-insulating phase in the large disorder limit. We observe that weak disorder suppresses the SF phase largely in the strong-coupling limit. Hence the region of the SF phase reduces in the presence of random on-site disorder. In the strong-coupling limit, based on the mapping to the hard-core Bose-Hubbard model, the system is expected to go from the SF phase to the Bose-glass phase. Blue circles denote the critical disorder determined by the scaling analysis for  $U/t = 5, 5.5,$  and  $6$ , respectively.

for higher values of the disorder strengths. Beyond the critical interaction, tuning of the disorder is expected to suppress the pair-pair correlations. In the strong-coupling limit ( $|U| \gg t$ ), the fermions exist in a bound state and hence the system can be described by a hard-core bosonic Hubbard model with repulsive next-nearest-neighbor interactions. As we expect that in the strong-coupling limit at noncommensurate integer filling ( $n = 0.5$ ), the hard-core Bose-Hubbard model shows a SF to BG transition [28]. Based on this mapping, we can expect our system to go from a SF to BG phase in the presence of disorder. We observe that weak disorder suppresses the SF phase largely in the strong-coupling limit, leading to the reduction of the SF region in the presence of random on-site disorder.

### IV. CONCLUDING REMARKS

In this paper, we have studied the bilayer BI model in the presence of disorder. Using the DQMC numerical technique, we have shown the effect of disorder on the KE and the double occupancy. We observe that the on-site random disorder plays a significant role in the localization of on-site pairs, and hence in the reduction of the effective hopping. This results in an increase in the double occupancy, which is an effect similar to the attractive interaction.

We also observe the existence of the long-range order in the pair-pair correlations at various disorder strengths. The random disorder does not affect the critical value of the interaction strength and the SF state survives even at intermediate disorder strengths. Finally, via finite-size scaling analysis, we have computed the critical disorder strength  $V_c \sim 1.44$ . For a single-layer attractive Hubbard model on a square lattice, previous QMC studies [24] reported  $V_c \sim 1.5$  at  $|U|/t = 4$ . In Table I, we have summarized the differences between the single-layer attractive Hubbard model with the bilayer band-insulator model studied here. In the single-layer AHM, the ground state is degenerate with the superfluid along with the CDW state for any finite interaction in the absence of disorder. Any finite amount of disorder removes this degeneracy with only the SF state in the ground state. At  $V_c$ , we observe the SF to BG transition. In the bilayer band-insulating model presented here, we have a BI to SF transition at finite interaction  $U_c$  in the absence of any disorder and there is no leading CDW order up to  $U = 10$ . In the presence of disorder, there is transition from a band-insulating to SF phase and from a SF to BG phase in the ground state.

Note that for large energy scale parameters  $t$ ,  $\beta$ , and  $U$ , small  $\Delta\tau$  is necessary for the accuracy of the Trotter-Suzuki decomposition [30]. Generally, the imaginary time steps are chosen such that  $\Delta\tau \leq \sqrt{0.25/U}$ . As  $U$  increases, one further need to decrease the imaginary time step, which further increases the running time of programs. The finiteness of  $\Delta\tau$  is a source of systematic errors. In this work, for practical purposes, the inverse temperature has been discretized in  $M = 200$  small imaginary time intervals  $\Delta\tau t = 0.05$ , which shows large fluctuations in two-particle correlations at large interaction regime (though disorder seems to destroy these fluctuations). For  $|U|/t = 8$ , we reduced the size of the imaginary time step to  $\Delta\tau t = 0.025$  by increasing the number of grids,  $M = 400$ .

TABLE I. Comparison of presented bilayer band-insulator model with single-layer attractive Hubbard model.

System	Single-layer model	Bilayer model
$V = 0$	Degenerate SF+CDW	BI to SF transition
$V \neq 0$	SF to BG transition	BI to SF transition; SF to BG transition

### ACKNOWLEDGMENTS

This work was supported by Ministry of Science, Republic of Korea through Grant No. NRF-2021R1111A2057259. Y.P. would like to acknowledge CSIR, India for financial support. Y.P. thanks A. V. Mallik, A. Halder, V. B. Shenoy,

and Nandini Trivedi for various discussions and comments. Y.P. would also like to thank V. B. Shenoy and H.P. Lee for the cluster usage for numerical calculations. H.L. acknowledges the hospitality at APCTP where part of this work was done.

- [1] P. W. Anderson, Theory of dirty superconductors, *J. Phys. Chem. Solids* **11**, 26 (1959).
- [2] N. Trivedi, R. T. Scalettar, and M. Randeria, Superconductor-insulator transition in a disordered electronic system, *Phys. Rev. B* **54**, R3756 (1996).
- [3] R. T. Scalettar, N. Trivedi, and C. Huscroft, Quantum Monte Carlo study of the disordered attractive Hubbard model, *Phys. Rev. B* **59**, 4364 (1999).
- [4] R. C. Dynes, J. P. Garno, G. B. Hertel, and T. P. Orlando, Tunneling study of superconductivity near the metal-insulator transition, *Phys. Rev. Lett.* **53**, 2437 (1984).
- [5] A. E. White, R. C. Dynes, and J. P. Garno, Destruction of superconductivity in quench-condensed two-dimensional films, *Phys. Rev. B* **33**, 3549 (1986).
- [6] A. A. Abrikosov and L. P. Gor'Kov, Superconducting alloys at finite temperatures, *Sov. Phys. J. Expt. Theor. Phys.* **36**, 319 (1959).
- [7] M. Ma and P. A. Lee, Localized superconductors, *Phys. Rev. B* **32**, 5658 (1985).
- [8] E. Orignac and T. Giamarchi, Effects of weak disorder on two coupled Hubbard chains, *Phys. Rev. B* **53**, R10453 (1996).
- [9] T. Paiva, E. Khatami, S. Yang, V. Rousseau, M. Jarrell, J. Moreno, R. G. Hulet, and R. T. Scalettar, Cooling atomic gases with disorder, *Phys. Rev. Lett.* **115**, 240402 (2015).
- [10] B. Damski, J. Zakrzewski, L. Santos, P. Zoller, and M. Lewenstein, Atomic Bose and Anderson glasses in optical lattices, *Phys. Rev. Lett.* **91**, 080403 (2003).
- [11] J. E. Lye, L. Fallani, M. Modugno, D. S. Wiersma, C. Fort, and M. Inguscio, Bose-Einstein condensate in a random potential, *Phys. Rev. Lett.* **95**, 070401 (2005).
- [12] D. Clément, A. F. Varón, J. A. Retter, L. Sanchez-Palencia, A. Aspect, and P. Bouyer, Experimental study of the transport of coherent interacting matter-waves in a 1D random potential induced by laser speckle, *New J. Phys.* **8**, 165 (2006).
- [13] M. Pasienski, D. McKay, M. White, and B. DeMarco, A disordered insulator in an optical lattice, *Nat. Phys.* **6**, 677 (2010).
- [14] J. Billy, V. Josse, Z. Zuo, A. Bernard, B. Hambrecht, P. Lugan, D. Clement, L. Sanchez-Palencia, P. Bouyer, and A. Aspect, Direct observation of Anderson localization of matter waves in a controlled disorder, *Nature (London)* **453**, 891 (2008).
- [15] B. Gadway, D. Pertot, J. Reeves, M. Vogt, and D. Schneble, Glassy behavior in a binary atomic mixture, *Phys. Rev. Lett.* **107**, 145306 (2011).
- [16] L. Fallani, J. E. Lye, V. Guarrera, C. Fort, and M. Inguscio, Ultracold atoms in a disordered crystal of light: Towards a Bose glass, *Phys. Rev. Lett.* **98**, 130404 (2007).
- [17] G. Roati, C. D'Errico, L. Fallani, M. Fattori, C. Fort, M. Zaccanti, G. Modugno, M. Modugno, and M. Inguscio, Anderson localization of a noninteracting Bose-Einstein condensate, *Nature (London)* **453**, 895 (2008).
- [18] D. Mitra, P. T. Brown, E. Guardado-Sanchez, S. S. Kondov, T. Devakul, D. A. Huse, P. Schauß, and W. S. Bakr, Quantum gas microscopy of an attractive Fermi-Hubbard system, *Nat. Phys.* **14**, 173 (2018).
- [19] M. Gall, C. F. Chan, N. Wurz, and M. Köhl, Simulating a Mott insulator using attractive interaction, *Phys. Rev. Lett.* **124**, 010403 (2020).
- [20] Y. Prasad, A. Medhi, and V. B. Shenoy, Fermionic superfluid from a bilayer band insulator in an optical lattice, *Phys. Rev. A* **89**, 043605 (2014).
- [21] Y. Prasad, Finite-temperature study of correlations in a bilayer band insulator, *Phys. Rev. B* **106**, 184506 (2022).
- [22] H. Lee, Y.-Z. Zhang, H. O. Jeschke, and R. Valentí, Competition between band and Mott insulators in the bilayer Hubbard model: A dynamical cluster approximation study, *Phys. Rev. B* **89**, 035139 (2014).
- [23] R. Rüger, L. F. Tocchio, R. Valentí, and C. Gros, The phase diagram of the square lattice bilayer Hubbard model: A variational Monte Carlo study, *New J. Phys.* **16**, 033010 (2014).
- [24] C. Huscroft and R. T. Scalettar, Effect of disorder on charge-density wave and superconducting order in the half-filled attractive Hubbard model, *Phys. Rev. B* **55**, 1185 (1997).
- [25] R. Blankenbecler, D. J. Scalapino, and R. L. Sugar, Monte Carlo calculations of coupled boson-fermion systems. I, *Phys. Rev. D* **24**, 2278 (1981).
- [26] R. R. dos Santos, Introduction to quantum Monte Carlo simulations for fermionic systems, *Braz. J. Phys.* **33**, 36 (2003).
- [27] D. A. Huse, Ground-state staggered magnetization of two-dimensional quantum Heisenberg antiferromagnets, *Phys. Rev. B* **37**, 2380 (1988).
- [28] M. P. A. Fisher, P. B. Weichman, G. Grinstein, and D. S. Fisher, Boson localization and the superfluid-insulator transition, *Phys. Rev. B* **40**, 546 (1989).
- [29] R. Mondaini, P. Nikolić, and M. Rigol, Mott-insulator to superconductor transition in a two-dimensional superlattice, *Phys. Rev. A* **92**, 013601 (2015).
- [30] Z. Bai, W. Chen, R. Scalettar, and I. Yamazaki, Numerical methods for quantum Monte Carlo simulations of the Hubbard model, *Multi-Scale Phenomena In Complex Fluids: Modeling, Analysis and Numerical Simulation* (World Scientific, 2009), pp. 1–110.